MIND THE UNCERTAINTY: GLOBAL PLATE MODEL CHOICE IMPACTS DEEP-TIME PALAEOBIOLOGICAL STUDIES

Lucas Buffan[1,2*], Lewis A. Jones[1*], Mathew Domeier[3], Christopher R. Scotese[4], Sabin Zahirovic[5], and Sara Varela[1]

[1]Centro de Investigación Mariña, Grupo de Ecoloxía Animal, Universidade de Vigo, 36310 Vigo, Spain

[2]Département de Biologie, École Normale Supérieure de Lyon, Université Claude Bernard Lyon 1, 69342 Lyon Cedex 07, France

[3]Centre for Earth Evolution and Dynamics (CEED), University of Oslo, NO-0316 Oslo, Norway

[4]Department of Earth and Planetary Sciences, Northwestern University, Evanston, Illinois 60208, USA

[5]EarthByte Group, School of Geosciences, University of Sydney, Sydney, NSW 2006, Australia

*These authors contributed equally to this work

Corresponding authors:

Lucas Buffan (Lucas.L.Buffan@gmail.com) and Lewis A. Jones (LewisAlan.Jones@uvigo.es)

Running headline: Palaeogeographic Uncertainty in Palaeobiology

Keywords: Coral reefs, Crocodiles, Global Plate Models, Macroecology, Palaeobiogeography, Palaeobiology, Palaeoclimate, Palaeogeography, Phanerozoic

Abstract

1. Global Plate Models (GPMs) aim to reconstruct the tectonic evolution of the Earth by modelling the motion of the plates and continents through time. These models enable palaeobiologists to study the past distribution of extinct organisms. However, different GPMs exist that vary in their partitioning of the Earth's surface and the modelling of continental motions. Consequently, the preferred use of one GPM will influence palaeogeographic reconstruction of fossil occurrences and any inferred palaeobiological and palaeoclimatic conclusion.
2. Here, using five open-access GPMs, we reconstruct the palaeogeographic distribution of cell centroids from a global hexagonal grid and quantify palaeogeographic uncertainty across the entire Phanerozoic (540–0 Ma). We measure uncertainty between reconstructed coordinates using two metrics: (1) palaeolatitudinal standard deviation and (2) mean pairwise geodesic distance. Subsequently, we evaluate the impact of GPM choice on palaeoclimatic reconstructions when using fossil occurrence data. To do so, we use two climatically-sensitive entities (coral reefs and crocodylomorphs) to infer the palaeolatitudinal extent of subtropical climatic conditions for the last 240 million years.
3. Our results indicate that differences between GPMs increase with the age of reconstruction. Specifically, cell centroids rotated to older intervals show larger differences in palaeolatitude and geographic spread than those rotated to younger intervals. However, high palaeogeographic uncertainty is also observed in younger intervals within tectonically complex regions (i.e. in the vicinity of terrane and plate boundaries). We also show that when using fossil data to infer the distribution of subtropical climatic conditions across the last 240 Ma, estimates vary by 6–7° latitude on average, and up to 24° latitude in extreme cases.
4. Our findings confirm that GPM choice is an important consideration when studying past biogeographic patterns and palaeoclimatic trends. We recommend using GPMs that report true

palaeolatitudes (through palaeomagnetic data use) and incorporating palaeogeographic uncertainty into palaeobiological analyses.

Introduction

Akin to neontologists, palaeobiologists seek to understand the origin, distribution, and extinction of species across time and space (e.g. Alroy, 2014; Powell et al., 2015; Spano et al., 2016; Meseguer and Condamine, 2020; Boddy et al., 2022). However, while neontologists can study the present-day geographic distribution of taxa, palaeobiologists must contend with the shift of the continents over geological timescales. Specifically, the geographic location of fossil occurrences on the Earth's surface today does not necessarily represent their location *in vivo*; fossil remains found at tropical latitudes might have been deposited at temperate latitudes, and vice versa. Consequently, reconstructing the past geographic distribution–i.e. the palaeogeographic distribution–of fossil occurrences is fundamental to the study of macroecological patterns in deep time. To do so, palaeobiologists routinely use what are known as Global Plate Models (e.g. Brocklehurst et al., 2017; Allen et al., 2020; Dunne et al., 2020; Antell et al., 2020; Boddy et al., 2022; Jones et al., 2022; Zhang et al., 2022).

Global Plate Models (GPMs) aim to reconstruct the tectonic evolution of the Earth, modelling the motion of the continents across its surface through geological time. They do so using Euler's rotation theorem to describe the motion of geometries–such as tectonic plates or geological terranes–on a sphere (McKenzie and Parker, 1967; Morgan, 1968). Since the 1970s, numerous GPMs have been developed by both the scientific community (e.g. Scotese et al., 1988; Müller et al., 1993, 2019; Golonka et al., 1994; Golonka, 2007; Torsvik et al., 2008a; Seton et al., 2012; Domeier and Torsvik, 2014; Matthews et al., 2016; Torsvik and Cocks, 2017; Scotese and Wright, 2018; Vérard, 2019; Young et al., 2019; Merdith et al., 2021) and industry (e.g. Getech plc and Robertson Research) for purposes such as geological resource exploration (Markwick, 2019) and Earth System modelling (Lunt et al., 2016). A more recent shift to 'full-plate models' (e.g. Merdith et al., 2021) and deforming plate models (e.g. Gurnis et al., 2018; Müller et al., 2019) has increased the complexity of GPMs by describing–in detail–

how plate boundaries, deforming regions, and the plate-mantle system have evolved through time (Seton et al., 2023).

A GPM is made up of two key components. The first component is a set of ‘geometries’ dividing the surface of the Earth into individual tectonic elements that can be independently reconstructed. These elements include both ‘dynamic polygons’ (also known as ‘continuously closing plate polygons’), which change shape through time, and ‘static polygons’, whose shape and size are fixed. The former are used to model entire tectonic plates, whereas the latter are used to delineate continents, fault-bound tectonic blocks (‘terranes’), or any other arbitrary parcel of crust whose shape and size can be treated as fixed through the modelled time. Whether any given continent or crustal block can be appropriately treated as a static polygon depends on the spatial resolution and timescale being considered, and so the number and definition of static polygons can vary significantly between GPMs (with more recent and temporally more extensive GPMs tending to have more static polygons), resulting in differential partitioning of the Earth’s surface (Fig. S1). Differences in the polygonization of the Earth’s surface between GPMs also arise from different interpretations about the locations of ancient tectonic boundaries—which occurs more frequently in complicated geological areas and in deeper time.

The second key component of a GPM is a rotation file that describes the time-dependent motion of the tectonic elements as finite (or “total”) Euler rotations (Müller et al., 2018; Domeier and Torsvik, 2019). These ‘rotation files’ can be read and interpolated by software programs such as ‘GPlates’ (Müller et al., 2018) to reconstruct the motion of the tectonic elements through time, and enable the reconstruction of palaeocoordinates for fossil occurrence data (Boyden et al., 2011; Wright et al., 2013). It is important to note that rotation files can report the motion of tectonic elements with respect to one another (‘relative’ motion) and/or with respect to the Earth’s mantle *or* the planetary spin-axis (so-called ‘absolute’ motion) (Torsvik et al., 2008a). Only the latter reference frame (the motion of tectonic elements relative to Earth’s spin axis) is appropriate for the reconstruction of fossil occurrence data as it reports true palaeolatitudes (Seton et al. 2023). Recent work has demonstrated differences in the palaeogeographic reconstruction of several fossil and geological datasets when using different GPMs (e.g. Cao et al., 2019; Boddy et al., 2022; Jones et al., 2022). Yet, the impact of model choice on palaeogeographic reconstructions at global Phanerozoic scale remains untested.

Quantifying this 'palaeogeographic uncertainty' is key to understanding the robustness of observed deep-time biodiversity patterns and their response to past climatic change (e.g. Mannion et al., 2014; Reddin et al., 2018). Here, we quantify spatial discrepancies in palaeogeographic reconstruction from five open-access GPMs. To do so, we reconstruct the palaeogeographic coordinates (i.e. palaeocoordinates) of centroids from a global hexagonal grid (~100 km spacing) across the last 540 million years (Myr). By comparing these five reconstructions, we identify key spatial zones and timeframes of palaeogeographic uncertainty. Subsequently, we reconstruct the palaeogeographic distribution of two climatically-sensitive entities (fossil coral reefs and terrestrial crocodylomorphs) to evaluate the impact of GPM choice on estimations of the palaeolatitudinal extent of tropical climatic conditions over the last 240 Myr. We hypothesise that: (1) differences in palaeogeographic reconstruction increase with age, and (2) GPM choice can significantly influence reconstructions of palaeogeographic distributions of organisms and inferred palaeoclimatic conditions.

Materials and Methods

Global Plate Models

Five open-access Global Plate Models (GPMs) were used to evaluate spatiotemporal differences in palaeogeographic reconstructions: WR13 (Wright et al., 2013), MA16 (Matthews et al., 2016), TC17 (Torsvik and Cocks, 2017), SC16 (Scotese, 2016; Scotese and Wright, 2018), and ME21 (Merdith et al., 2021). These GPMs have variable temporal coverage (see Table 1) with WR13, SC16, TC17, and ME21 covering the entirety of our Phanerozoic study period (540–0 Ma), while MA16 is limited to the Devonian–Recent (410–0 Ma).

Table 1: A summary table of the Global Plate Models used in this study. The table includes the abbreviations used in this study, the names of models according to the GPlates Web Service (https://gwsdoc.gplates.org), the temporal coverage of each model, and the relevant reference for each model.

Abbreviation	GPlates ID	Temporal coverage	Reference
WR13	GOLONKA	0–550 Ma	(Wright et al., 2013)
MA16	MATTHEWS2016_pmag_ref	0–410 Ma	(Matthews et al., 2016)
TC17	TorsvikCocks2017	0–540 Ma	(Torsvik and Cocks, 2017)
SC16	PALEOMAP	0–1100 Ma	(Scotese, 2016; Scotese and Wright, 2018)
ME21	MERDITH2021	0–1000 Ma	(Merdith et al., 2021)

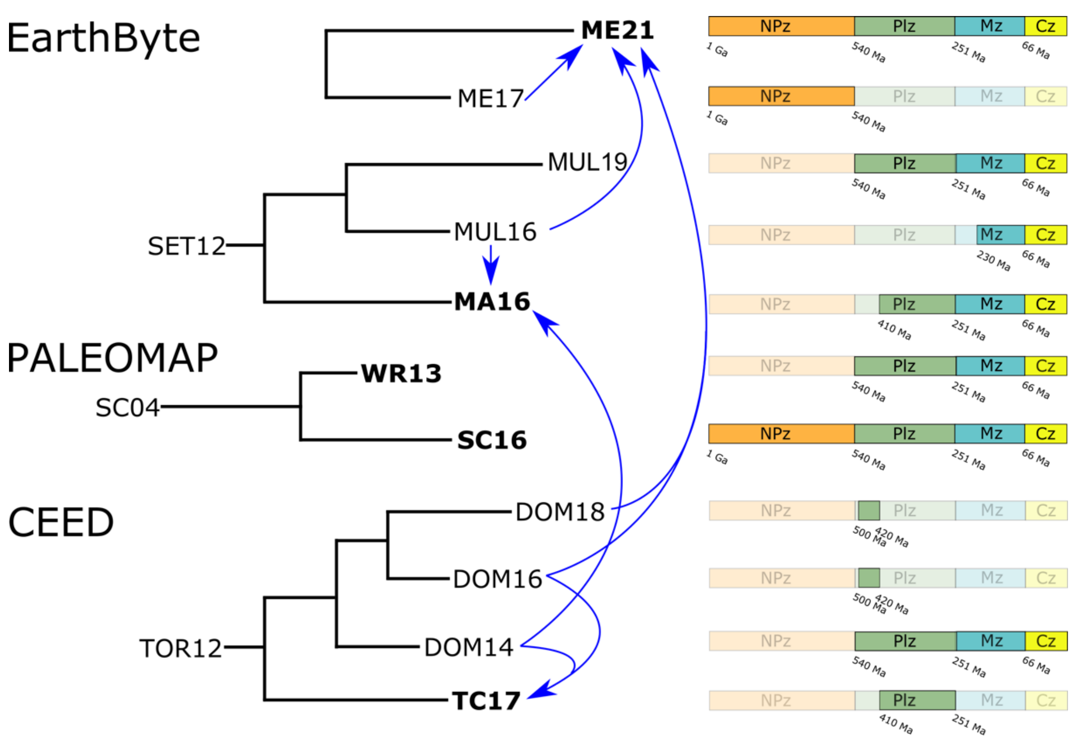

Figure 1: A ‘cladogram’-type representation of the relationship between Global Plate Models from the three main model development groups (EarthByte, PALEOMAP project, and Centre for Earth Evolution and Dynamics (CEED)) used in this study, and their respective temporal coverage. Blue arrows indicate ‘horizontal transfers’ between models, i.e. amalgamations of models from different

groups. Global Plate Model abbreviations: TOR12 (Torsvik et al., 2012), DOM14 (Domeier and Torsvik, 2014), TC17 (Torsvik and Cocks, 2017), DOM16 (Domeier, 2016), DOM18 (Domeier, 2018), MA16 (Matthews et al., 2016), ME17 (Merdith et al., 2017), ME21 (Merdith et al., 2021), MUL16 (Müller et al., 2016), MUL19 (Müller et al., 2019), SC04 (Scotese, 2004), SC16 (Scotese, 2016; Scotese and Wright, 2018), SET12 (Seton et al., 2012), WR13 (Wright et al., 2013). Models included in this study are represented in bold. Era abbreviations: Cenozoic (Cz), Mesozoic (Mz), Palaeozoic (Plz), and Neo-Proterozoic (NPz).

WR13 and SC16 both share a common lineage stemming from the plate model of Scotese (2004), but WR13 employed modifications to fit palaeomagnetic data summarised in (Torsvik and Van der Voo, 2002), whereas SC16 was used to produce the widely-used set of Phanerozoic paleogeographic maps and digital elevation models (Scotese and Wright, 2018). The Scotese GPM has evolved slowly over the last three decades. Small, but significant, changes have occurred in the location of the core continents (e.g. North America, Europe, Gondwana), whereas major changes have occurred in the placement of N. China, S. China, Cimmeria, and the exotic terranes of western North America (Fig. S2). The time range of the Scotese GPM has also been extended further into the Precambrian (Scotese, 2004, 2016; Scotese and Elling, 2017). TC16 primarily stems from the global paleomagnetic model of Torsvik et al. (2012), but it incorporates some changes made in the subsequent plate models of Domeier and Torsvik (2014) for the late Palaeozoic (410–250 Ma), and Domeier (2016) in the earlier Palaeozoic (500–410 Ma). Note that TC16 is presented in a mantle reference frame by default, but here we use the version which is available in the paleomagnetic reference frame. The model of MA16 is likewise built upon the model of Domeier and Torsvik (2014) for the late Paleozoic (410–250), and so MA16 and TC16 are very similar for that interval of time. For Mesozoic and Cenozoic time, MA16 is based on the model of Müller et al. (2016). Note that the model of Müller et al. (2016) exists in a mantle reference frame, and so too does the original model of MA16 for times between 250 and 0 Ma. However, a version cast into the paleomagnetic reference frame was subsequently made available, using the global apparent polar wander path from Torsvik et al. (2012), and here we utilize this later version. ME21 is largely a composition of several pre-existing models, namely the model of Merdith et al. (2017) from 1000–500 Ma, the models of Domeier (2016; 2018) for the early Palaeozoic (500–410 Ma), and a modified version of Young et al. (2019) for the interval 410–0 Ma, and the entire 1000–0 Ma model interval is cast into a paleomagnetic reference frame. The model of Young et al. (2019) is modified from Matthews et al. (2016), which again was built from Domeier and Torsvik (2014) for the late Palaeozoic interval (410–250 Ma) and Müller et al. (2016) from 230–0 Ma. Thus, for the Palaeozoic interval (particularly the late Palaeozoic), there is some common ancestry between TC16, MA16 and ME21, and this extends into the Mesozoic and Cenozoic for MA16 and ME21. Nevertheless, the modifications made between these alternative models is a reflection of outstanding paleogeographic uncertainty. Figure 1 summarises the main interrelationships between these various GPMs.

Quantifying spatiotemporal differences

To quantify differences in palaeogeographic reconstruction (Fig. 1), we first generated a discrete global hexagonal grid (~100 km spacings) via the python library 'h3' v.3.7.6 (Uber, 2023). Most GPMs have a network of static polygons covering most of the Earth's continental areas, and we retained only the grid cells that were included within a static polygon in each of the GPMs. Subsequently, we reconstructed palaeocoordinates for cell centroids across the last 540 Myr with a timestep of 10 Myr for each GPM, resulting in up to 54 time steps depending on GPM (Table 1). To do so, we used the python library 'pygplates' ver. 0.36.0 (Williams et al., 2017) to interact with the software GPlates (Boyden et al., 2011; Müller et al., 2018). Using the reconstructed palaeocoordinates for each cell–from each model–we calculated: (1) the standard deviation (SD) in palaeolatitude and (2) the mean pairwise geodesic distance (PGD) between reconstructed coordinates (up to five sets) for each cell. The former of these quantifies the potential uncertainty in palaeolatitude between models with significance for studies such as those focused on reconstructing the latitudinal biodiversity gradients in deep time (e.g. Allen et al., 2020; Song et al., 2020). The latter quantifies the uncertainty in palaeogeographic position between models having significance for studies focused on themes such as reconstructing organisms' geographic range sizes (e.g. Antell et al., 2020). Mean PGD was calculated using the R package 'geosphere' ver. 1.5-18 (Hijmans et al., 2021).

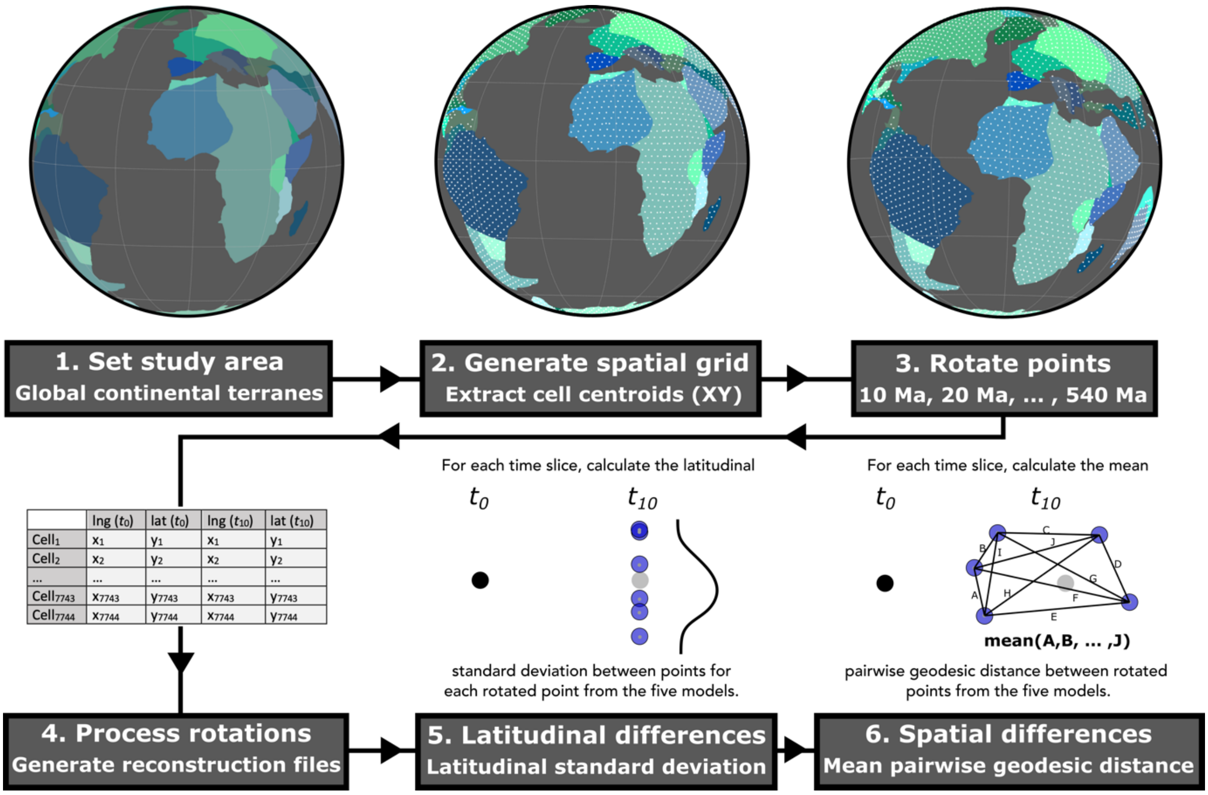

Figure 2: A graphical schematic of the simulation workflow used in this study. Using continental tectonic elements, the study area is first established (1). Subsequently, a discrete global hexagonal grid (~100 km spacings) is generated via the python library 'h3' v.3.7.6 (Uber, 2023) and cell centroids extracted for cells intersecting with the continental tectonic elements (2). Cell centroids are then rotated (3) at time intervals of 10 Myr throughout the Phanerozoic (540–0 Ma), for each model, using the software GPlates via the 'pygplates' ver. 0.36.0 python library (Williams et al., 2017). Reconstruction files are subsequently generated for each model (4), and the palaeolatitudinal standard deviation (5) and the mean pairwise geodesic distance (6) calculated for each cell centroid between the five models for each time step.

Palaeoclimatic reconstruction

To test the influence of GPM choice on fossil-based palaeoclimatic reconstructions, we estimate the palaeolatitudinal extent of (sub-)tropical climatic conditions using two climatically sensitive entities: warm-water coral reefs and terrestrial crocodylomorphs. These entities are frequently used to infer the extent of (sub-)tropical palaeoclimatic conditions due to their limited thermal tolerance and geographic distribution today (e.g. Markwick, 2007; Burgener et al., 2023). Fossil crocodylomorph occurrences (="Crocodylomorpha") were downloaded from The Paleobiology Database (https://paleobiodb.org/#/) on the 9th of November 2022 and were restricted to terrestrial taxa and body fossils. Marine taxa were excluded as they appear to be less constrained by climatic factors than terrestrial taxa (Mannion et al., 2015). Fossil coral reef occurrences were downloaded from the PaleoReef Database (Kiessling and Krause, 2022) on the 10th of March 2022 and were restricted to scleractinian 'true reefs' with a tropical affinity. This led us to exclude pre-Anisian reef occurrences. At the end of the cleaning, the midpoint age of oldest crocodylomorph occurrence was 232.5 Ma, and the oldest reef occurrence was 231.5 Ma. Finally, fossil occurrences were split into 10 Myr time bins using the midpoint age of each occurrence's age range. After data processing, 4638 terrestrial crocodylomorphs and 419 warm-water coral reef occurrences remained for analyses.

Using the five GPMs (Table 1), we reconstructed the palaeocoordinates for each occurrence based on the midpoint of its respective age range. Assuming hemispheric symmetry in climatic conditions, we subsequently identified the maximum absolute palaeolatitude within each time bin–for each model and entity–to infer the palaeolatitudinal extent of (sub-)tropical climatic conditions. Using this deduction, we quantified the potential uncertainty in the palaeolatitudinal extent of (sub-)tropical climatic conditions by calculating the palaeolatitudinal range between estimates for each time bin. Finally, for each fossil occurrence, we calculated the median, maximum and minimum reconstructed palaeolatitude from the five model estimates.

Results

Spatiotemporal discrepancy trends

Palaeolatitudinal SD and mean PGD demonstrate an increasing uncertainty in palaeogeographic reconstruction with age (Fig. 3–4; Fig. S3). Overall, GPMs are in good agreement for the last 100 Myr (mid-Cretaceous–Recent), with 97.4% of cells having a palaeolatitudinal SD less than 5º and a mean PGD less than 1000 km (Fig. 3). However, GPM reconstructions begin to substantially diverge at greater reconstruction ages with generally increasing uncertainty throughout the Mesozoic (251.9–66 Ma) and Palaeozoic (538.8–251.9 Ma). For example, in the Cenozoic (66–0 Ma), 1.9% of cells have a palaeolatitudinal SD of more than 5º, going up to 14.8% of cells during the Mesozoic, and 53.8% during the Palaeozoic (Fig. 3a). This trend is further reflected by an increase in mean PGD with 1.2% of cells having a value of more than 1000 km in the Cenozoic, 20.2% during the Mesozoic, and 80% during the Palaeozoic (Fig. 3b). Differences in Cambrian (538.8–485.4 Ma) reconstructions are especially large, with a considerable proportion of cells having a palaeolatitudinal SD of more than 5º (~76.3%) and mean PGD of more than 1000 km (~90.1%) (Fig. 3; Fig. S3). Notably, despite this overall trend of increasing palaeogeographic uncertainty with age, uncertainty is relatively low during the latest Carboniferous and Permian in comparison to the rest of the Palaeozoic and early Mesozoic (Fig. 3).

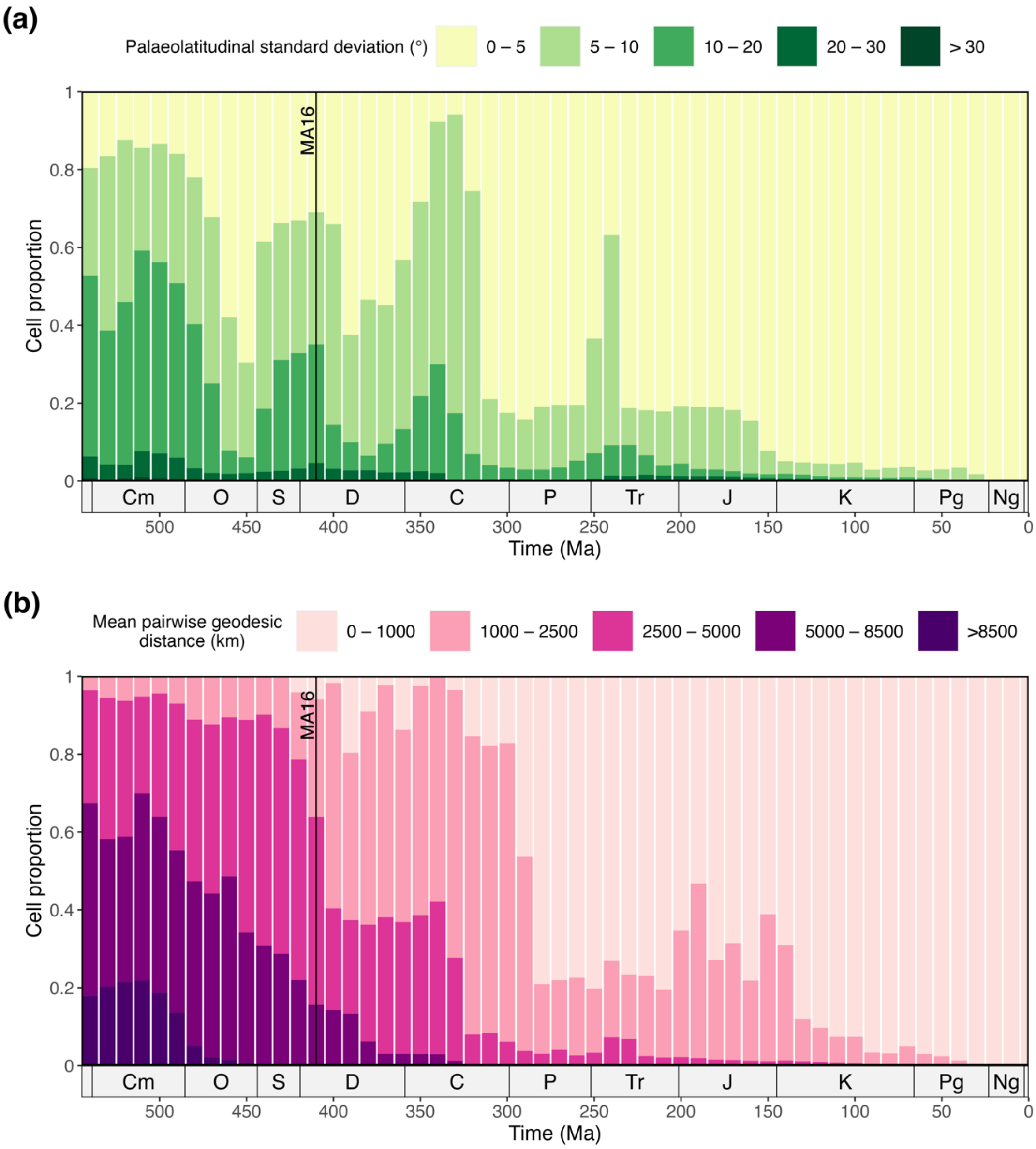

Figure 3: Phanerozoic trends in spatial discrepancies between Global Plate Models within 10 Myr time steps. Values are categorised and depicted as proportions of cells. (a) Palaeolatitudinal standard deviation between reconstructed palaeocoordinates for cell centroids. (b) Mean pairwise geodesic distance between reconstructed palaeocoordinates for cell centroids. The black line depicts the temporal limit (410 Ma) of the MA16 model (Matthews et al., 2016). The bar plots show increasing palaeogeographic uncertainty between models with age of reconstruction. Period abbreviations are as follows: Cambrian (Cm); Ordovician (O), Silurian (S), Devonian (D), Carboniferous (C), Permian (P),

Triassic (Tr), Jurassic (J), Cretaceous (K), Paleogene (Pg), and Neogene (Ng). The Quaternary is not depicted. The Geological Time Scale axis was added to the plot using the R package ‘deeptime’ ver. 1.0.1 (Gearty, 2023).

Our palaeolatitudinal SD and mean PGD results show palaeogeographic uncertainty is not evenly distributed in space (Fig. 4; Fig. S3). High palaeogeographic uncertainty is generally restricted to plate boundaries and active deformation zones during the Cenozoic and Mesozoic but extends to broader areas during the Palaeozoic (Fig. 4; Fig. S3; supplementary GIFs). For example, throughout the Cenozoic and Mesozoic, palaeogeographic reconstructions of South American cell centroids appear well constrained in comparison to those along the Eurasian-Indian and Eurasian-Arabian plate boundaries (Fig. 4; Fig. S3; supplementary GIFs).

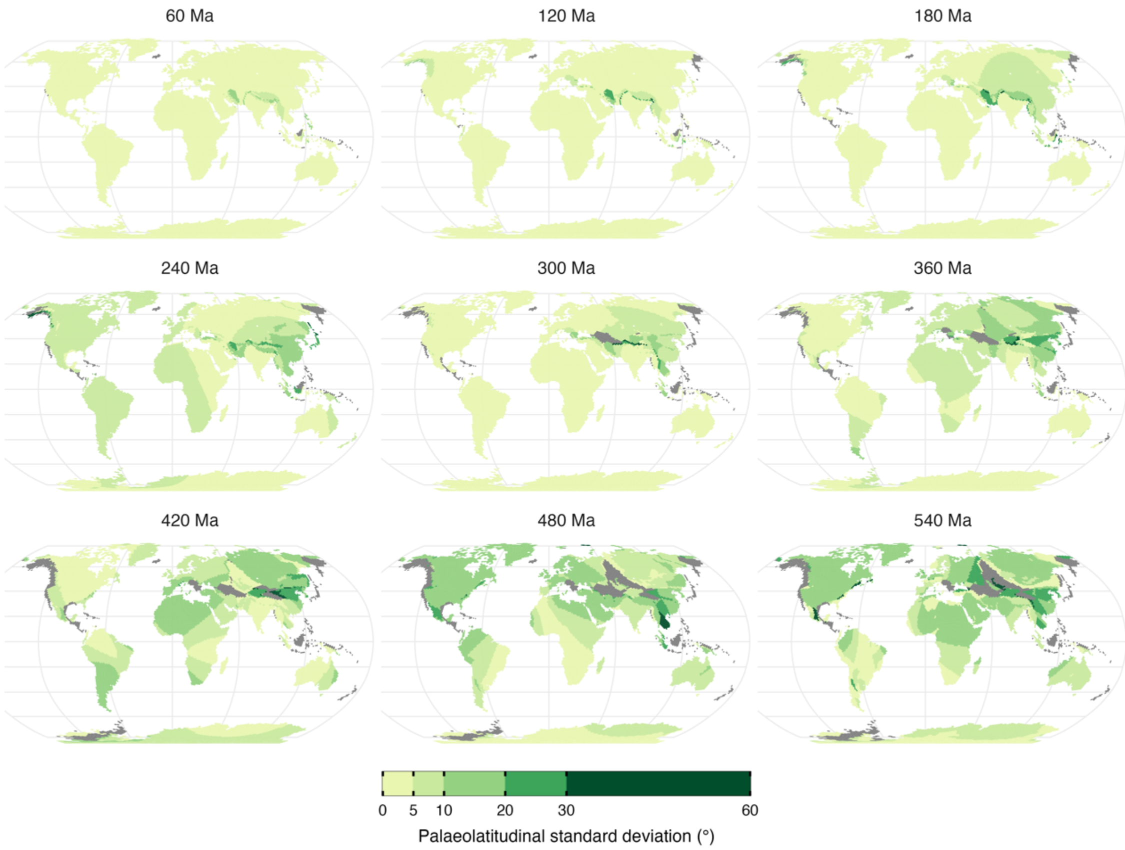

Figure 4: Categorised maps of the palaeolatitudinal standard deviation between reconstructed palaeocoordinates of cell centroids from Global Plate Models. Values are mapped onto a present-day

map with darker shades indicating greater palaeolatitudinal standard deviation between palaeocoordinates. Grey cells denote areas where palaeocoordinates could not be reconstructed at time of reconstruction for cell centroids by at least two models. Maps are presented in the Robinson projection (ESRI:54030).

Palaeoclimatic reconstructions

Our results suggest that reconstructions of the palaeolatitudinal extent of (sub-)tropical climatic conditions–based on terrestrial crocodylomorphs and coral reef occurrences–can vary by up to 12.3º latitude in crocodylomorphs and 24.1º in coral reefs, depending on GPM choice (Fig. 5). The average range between models along the 240 Myr time series is 7.7º for coral reefs and 6.5º for terrestrial crocodylomorphs (Fig. 5). However, despite these large observed differences, the direction of change (equatorward vs. poleward) in the extent of (sub-)tropical conditions is largely consistent between GPMs (Fig. 5). Both time series exhibit a significant positive correlation between age of reconstruction and the range in the extent of (sub-)tropical conditions from GPM estimates (Pearson's correlation test: $R = 0.43$; $P = 0.05$ for coral reefs and $R = 0.55$; $P = 0.005$ for crocodylomorphs). Comparisons of reconstructed palaeocoordinates for all occurrences further support an increase in palaeolatitudinal uncertainty with age (Fig. S5). For example, the average palaeolatitudinal range between the five GPMs for each occurrence–within each time bin–increases significantly with age (Pearson's correlation test: $R = 0.49$; $P < 0.001$ for coral reefs and $R = 0.33$; $P < 0.001$ for crocodylomorphs).

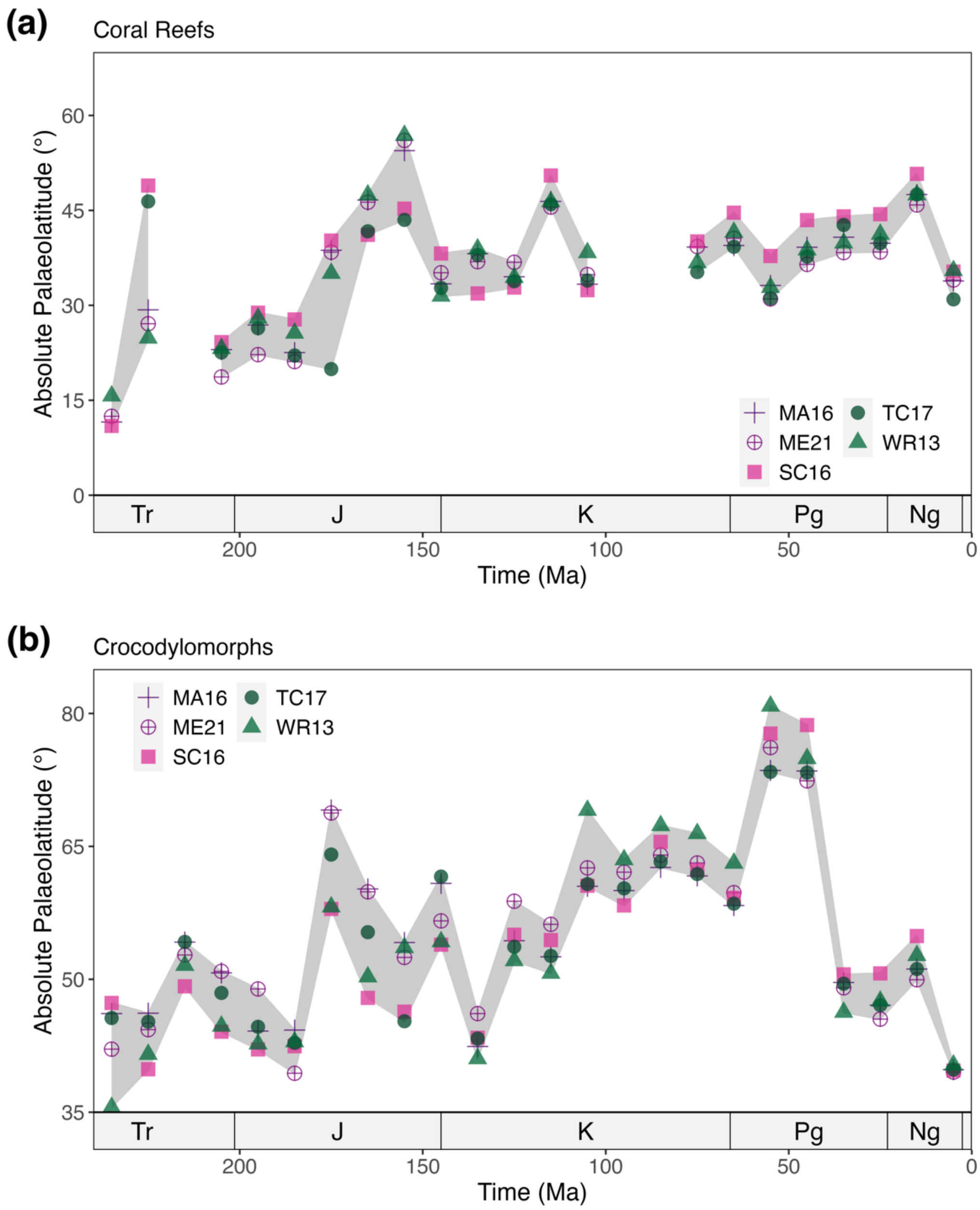

Figure 5: Palaeogeographic uncertainty in fossil-based reconstruction of the (sub-)tropics within 10 Myr time steps (0–240 Ma). For each time step, the maximum absolute reconstructed palaeolatitude of coral reefs with a tropical affinity (a) and terrestrial crocodylomorphs (b) is depicted for each Global Plate Model. The uncertainty of the palaeolatitudinal limit of subtropical reconstruction is depicted as the range between the maximum absolute palaeolatitudes (grey ribbon), with an average uncertainty of 7.7° for coral reefs (a) and 6.5° for crocodylomorphs (b). Both time series exhibit a strong positive

correlation between age of reconstruction and palaeolatitudinal uncertainty (R = 0.43–0.55; $P \leq 0.05$). Global Plate Model abbreviations are the same as in Figure 1. The Geological Time Scale axis was added to the plot using the R package 'deeptime' ver. 1.0.1(Gearty, 2023).

Discussion

With age comes uncertainty

In this study, we quantified palaeogeographic reconstruction differences between five Global Plate Models (GPMs). Our results demonstrate that palaeogeographic uncertainty increases with age (Fig. 3) suggesting caution is required when reconstructing deep-time macroecological trends such as geographic range sizes (e.g. Antell et al., 2020), latitudinal biodiversity gradients (e.g. Powell, 2009; Zhang et al., 2022), and organisms' spatial response to global climatic change (e.g. Reddin et al., 2018). However, the issue of palaeogeographic uncertainty also has relevance for fields such as palaeoclimatology, where palaeotemperature proxies are used to reconstruct latitudinal temperature gradients (e.g. Zhang et al., 2019) and evaluate the performance of palaeoclimatic simulations (e.g. Lunt et al., 2021). Therefore, in the wake of additional methodological concerns that have been considered recently–e.g. spatial sampling bias in the geological record (e.g. Vilhena and Smith, 2013; Close et al., 2020; Jones and Eichenseer, 2021)–our work raises a new challenge for those working with fossil data in deep time. Following our results, we recommend that studies dealing with deep time palaeogeographic reconstructions should consider the robustness of their conclusions to GPM choice (e.g. Boddy et al., 2022), particularly for intervals older than ~300 Ma. Moreover, akin to phylogenies, we advocate that reconstructed coordinates should be treated as the model-based estimates they are, rather than empirical data.

Spatial clusters of palaeogeographic uncertainty

Our results show that palaeogeographic reconstruction discrepancies are not only uneven in time, but also in space. During the Cenozoic and Mesozoic, high palaeogeographic uncertainty is clustered around active plate boundaries and tectonically complex regions such as along the Eurasian-Indian, Eurasian-Arabian, and North American-Juan de Fuca plate boundaries (Fig. 4; Fig. S3). The high uncertainty values found in these areas is a direct result of differential partitioning in GPMs with cell centroids assigned to different geometries, each with their own unique reconstruction history (Fig. S1). This finding suggests that additional caution is warranted when reconstructing the palaeogeographic distribution of fossil occurrences originating from areas close to plate boundaries or within tectonically complex regions. Hence, reconstructions of fossil occurrences from cratonic areas–stable interior portions of continents–ought to be more consistent between GPMs than reconstructions of fossil occurrences from continental margins or the edges of tectonic blocks. However, our results also suggest that there is an overarching trend of increasing uncertainty among GPMs throughout the Palaeozoic, even in cratonic areas. Rather than differences in the delineation of static polygons, this reflects differences in the modelled rotation histories as prescribed by the rotation files.

Pre-Jurassic palaeolongitudinal uncertainty

The direct reconstruction of palaeolongitude is challenging for most of Earth's history. While palaeomagnetic data can be used to constrain the relative palaeolatitudinal position of plates and continents, they cannot directly constrain palaeolongitude (Vérard, 2019). Hotspot tracks, which record the motion of a tectonic plate over a mantle plume, enable the determination of palaeolongitude (with respect to the base of the mantle), but owing to the incessant recycling of oceanic crust, well-resolved hotspot tracks are limited to the last ~130 Ma (Seton et al. 2023). Marine magnetic anomalies enable the determination of relative palaeolongitude back to the time of Pangaea breakup (~200 Ma), but they cannot constrain absolute palaeolongitude. Other attempts to constrain palaeolongitude in deeper time remain controversial (Torsvik et al., 2008b; Mitchell et al., 2012). This has broad implications for palaeobiological studies such as those reconstructing organisms' geographic range sizes in deep time (e.g. Kiessling and Aberhan, 2007). However, this will only be an issue in cases where occurrences span a relatively wide number of terranes. Nevertheless, one should also bear in mind that the palaeolatitudinal distribution of the continents can also vary significantly between GPMs particularly in the Palaeozoic (Fig. S4), likely resulting from increasing sparsity of palaeomagnetic data over that period, as shown by Torsvik et al. (2012).

Reconstructing palaeoclimatic conditions

Fossil occurrences of climatically-sensitive organisms are routinely used to estimate the distribution of past climatic conditions (e.g. Frakes et al., 1992; Scotese et al., 2021; Burgener et al., 2023). Here–using five different GPMs–we estimated the palaeolatitudinal extent of (sub-)tropical climatic conditions for the last 240 Myr using fossil terrestrial crocodylomorphs and warm-water coral reefs (Fig. 5). Our findings support previous work in demonstrating that GPM choice can strongly influence reconstructions of palaeoclimatic conditions when based on geological data (e.g. Cao et al., 2019). Moreover, our results suggest that previous conclusions based on the use of one GPM might be worth revisiting (e.g. Markwick, 1998; Kiessling, 2001). Nevertheless, while large differences (~24.1º latitude) can be observed between GPMs in extreme cases, the direction of change (equatorward vs. poleward) is largely consistent between GPMs suggesting broad-scale relative patterns are constrained. Consequently–across temporal scales–the use of a single GPM can be useful for informing relative changes within a time series, but the magnitude of change relative to the present-day should be carefully considered.

Study limitations

We quantified Phanerozoic (540–0 Ma) palaeogeographic uncertainty between five GPMs using a global hexagonal grid (~100 km spacings). While the use of additional models such as the commonly applied Getech plate model would be desirable to further quantify palaeogeographic uncertainty (e.g. Chiarenza et al., 2019; Saupe et al., 2019), not all GPMs are open access and broadly available to the community. Despite this, the use of additional models is unlikely to change the general trends observed in this study which are primarily driven by limited data availability (e.g. palaeomagnetic data and constraints on palaeolongitude) and geological interpretation (e.g. tectonic boundaries). Furthermore, the spatial resolution of our study (~100 km spacings) may influence our results in the identification of areas of high palaeogeographic uncertainty. For example, along geological boundaries, a finer-scale grid might further constrain the areal extent of these areas. Nevertheless, our results provide a first-order advisory note for those working with spatial data and advocates for the quantification of palaeogeographic uncertainty for individual datasets.

Conclusion

In conclusion, our study demonstrates that differences in palaeogeographic reconstruction increase with age. Consequently, an increasing level of caution is warranted when reconstructing fossil assemblages from older intervals, particularly for intervals older than ~300 Ma. Nevertheless, consideration is also required–even for younger intervals–for fossil occurrences originating from tectonically complex regions where the definition of tectonic boundaries lack consensus between Global Plate Models. Our study also demonstrates the impact Global Plate Model choice can have on broader conclusions such as reconstructions of palaeoclimatic conditions based on fossil occurrence data. Therefore, we endorse that studies dependent on deep-time palaeogeographic reconstructions should only use models based on a palaeomagnetic reference frame to reconstruct fossil palaeocoordinates, test the sensitivity of their conclusions to Global Plate Model choice, and quantify the palaeogeographic uncertainty associated with their data.

Acknowledgements

We are grateful for the efforts of all those who have contributed to collecting the fossil data used in this study and entering them into the Paleobiology Database and the PaleoReefs Database. L.B. was funded by the École Normale Supérieure de Lyon, France. L.A.J. and S.V. were funded by the European Research Council under the European Union's Horizon 2020 research and innovation program (grant agreement 947921) as part of the MAPAS project. L.A.J. was also supported by a Juan de la Cierva-formación 2021 fellowship (FJC2021-046695-I) funded by MCIN/AEI/10.13039/501100011033 and the European Union NextGenerationEU/PRTR. SZ was supported by Australian Research Council grant DE210100084. (py)GPlates development is funded by the AuScope National Collaborative

Research Infrastructure System (NCRIS) program. This is Palaeobiology Database publication no XXX.

Authors' contributions

LAJ and SV conceived the project. All authors contributed to developing the project. LB, LAJ and MD wrote the code, conducted the analyses, and produced the figures. All authors contributed to writing the manuscript.

Data availability

The data generated in this study have been included within the paper, its supplementary material, and dedicated GitHub repository (https://github.com/Buffan3369/rotation_sensitivity).

Code availability

Generation of the reconstruction grids and palaeocoordinates for fossil occurrence data were generated via pygplates run in python version 3.9.7. All data analyses were conducted in R version 4.2.2. The workflow is available both as R scripts and Jupyter notebooks on GitHub (accessible via: https://github.com/Buffan3369/rotation_sensitivity).

References

Allen, B.J., Wignall, P.B., Hill, D.J., Saupe, E.E., and Dunhill, A.M., 2020, The latitudinal diversity gradient of tetrapods across the Permo-Triassic mass extinction and recovery interval: Proceedings of the Royal Society B: Biological Sciences, v. 287, doi:10.1098/rspb.2020.1125.

Alroy, J., 2014, Accurate and precise estimates of origination and extinction rates: Paleobiology, v. 40, p. 374–397, doi:10.1666/13036.

Antell, G.S., Kiessling, W., Aberhan, M., and Saupe, E.E., 2020, Marine Biodiversity and Geographic Distributions Are Independent on Large Scales: Current Biology, v. 30, p. 115- 121.e5, doi:10.1016/j.cub.2019.10.065.

Boddy, C.E., Mitchell, E.G., Merdith, A., and Liu, A.G., 2022, Palaeolatitudinal distribution of the Ediacaran macrobiota: Journal of the Geological Society, v. 179, p. jgs2021- 030, doi:10.1144/jgs2021-030.

Boyden, J.A., Müller, R.D., Gurnis, M., Torsvik, T.H., Clark, J.A., Turner, M., Ivey-Law, H., Watson, R.J., and Cannon, J.S., 2011, Next-generation plate-tectonic reconstructions using GPlates, *in*

Geoinformatics: Cyberinfrastructure for the Solid Earth Sciences, Cambridge, Cambridge University Press, p. 95–113.

Brocklehurst, N., Day, M.O., Rubidge, B.S., and Fröbisch, J., 2017, Olson's extinction and the latitudinal biodiversity gradient of tetrapods in the Permian: Proceedings of the Royal Society B: Biological Sciences, v. 284, p. 1–8.

Burgener, L., Hyland, E., Reich, B.J., and Scotese, C., 2023, Cretaceous climates: Mapping paleo-Köppen climatic zones using a Bayesian statistical analysis of lithologic, paleontologic, and geochemical proxies: Palaeogeography, Palaeoclimatology, Palaeoecology, v. 613, p. 111373, doi:10.1016/j.palaeo.2022.111373.

Cao, W., Williams, S., Flament, N., Zahirovic, S., Scotese, C., and Müller, R.D., 2019, Palaeolatitudinal distribution of lithologic indicators of climate in a palaeogeographic framework: Geological Magazine, v. 156, p. 331–354, doi:10.1017/S0016756818000110.

Chiarenza, A.A., Mannion, P.D., Lunt, D.J., Farnsworth, A., Jones, L.A., Kelland, S.-J., and Allison, P.A., 2019, Ecological niche modelling does not support climatically-driven dinosaur diversity decline before the Cretaceous/Paleogene mass extinction: Nature Communications, v. 10, p. 1–14, doi:10.1038/s41467-019-08997-2.

Close, R.A., Benson, R.B.J., Saupe, E.E., Clapham, M.E., and Butler, R.J., 2020, The spatial structure of Phanerozoic marine animal diversity: Science, v. 368, p. 420–424, doi:10.1126/science.aay8309.

Domeier, M., 2016, A plate tectonic scenario for the Iapetus and Rheic oceans: Gondwana Research, v. 36, p. 275–295, doi:10.1016/j.gr.2015.08.003.

Domeier, M., 2018, Early Paleozoic tectonics of Asia: Towards a full-plate model: Geoscience Frontiers, v. 9, p. 789–862, doi:10.1016/j.gsf.2017.11.012.

Domeier, M., and Torsvik, T.H., 2019, Full-plate modelling in pre-Jurassic time: Geological Magazine, v. 156, p. 261–280.

Domeier, M., and Torsvik, T.H., 2014, Plate tectonics in the late Paleozoic: Geoscience Frontiers, v. 5, p. 303–350, doi:10.1016/j.gsf.2014.01.002.

Dunne, E.M., Farnsworth, A., Greene, S.E., Lunt, D.J., and Butler, R.J., 2020, Climatic drivers of latitudinal variation in Late Triassic tetrapod diversity: Palaeontology, v. 64, p. 101–117, doi:https://doi.org/10.1111/pala.12514.

Frakes, L.A., Francis, J.E., and Syktus, J.I., 1992, Climate Modes of the Phanerozoic: Cambridge, Cambridge University Press, doi:10.1017/CBO9780511628948.

Gearty, W., 2023, deeptime: Plotting Tools for Anyone Working in Deep Time. R package version 1.0.1.:, https://CRAN.R-project.org/package=deeptime.

Golonka, J., 2007, Late Triassic and Early Jurassic palaeogeography of the world: Palaeogeography, Palaeoclimatology, Palaeoecology, v. 244, p. 297–307.

Golonka, J.R., Ross, M.I., and Scotese, C.R., 1994, Phanerozoic paleogeographic and paleoclimatic modeling maps: Pangea: Global Environments and Resources, v. 17, p. 1–47.

Gurnis, M., Yang, T., Cannon, J., Turner, M., Williams, S., Flament, N., and Müller, R.D., 2018, Global tectonic reconstructions with continuously deforming and evolving rigid plates: Computers & Geosciences, v. 116, p. 32–41, doi:10.1016/j.cageo.2018.04.007.

Hijmans, R.J., Karney (GeographicLib), C., Williams, E., and Vennes, C., 2021, geosphere: Spherical Trigonometry:, https://CRAN.R-project.org/package=geosphere (accessed February 2022).

Jones, L.A., and Eichenseer, K., 2021, Uneven spatial sampling distorts reconstructions of Phanerozoic seawater temperature: Geology, doi:10.1130/G49132.1.

Jones, L.A., Mannion, P.D., Farnsworth, A., Bragg, F., and Lunt, D.J., 2022, Climatic and tectonic drivers shaped the tropical distribution of coral reefs: Nature Communications, v. 13, p. 3120, doi:10.1038/s41467-022-30793-8.

Kiessling, W., 2001, Paleoclimatic significance of Phanerozoic reefs: Geology, v. 29, p. 751–754, doi:10.1130/0091-7613(2001)029<0751:PSOPR>2.0.CO;2.

Kiessling, W., and Aberhan, M., 2007, Geographical distribution and extinction risk: lessons from Triassic–Jurassic marine benthic organisms: Journal of Biogeography, v. 34, p. 1473–1489, doi:10.1111/j.1365-2699.2007.01709.x.

Kiessling, W., and Krause, M.C., 2022, PARED - An online database of Phanerozoic reefs: PARED - An online database of Phanerozoic reefs, https://www.paleo-reefs.pal.uni-erlangen.de (accessed October 2021).

Lunt, D.J. et al., 2021, DeepMIP: model intercomparison of early Eocene climatic optimum (EECO) large-scale climate features and comparison with proxy data: Climate of the Past, v. 17, p. 203–227, doi:10.5194/cp-17-203-2021.

Lunt, D.J., Farnsworth, A., Loptson, C., Foster, G.L., Markwick, P., O'Brien, C.L., Pancost, R.D., Robinson, S.A., and Wrobel, N., 2016, Palaeogeographic controls on climate and proxy interpretation: Climate of the Past, v. 12, p. 1181–1198, doi:10.5194/cp-12-1181-2016.

Mannion, P.D., Benson, R.B.J., Carrano, M.T., Tennant, J.P., Judd, J., and Butler, R.J., 2015, Climate constrains the evolutionary history and biodiversity of crocodylians: Nature Communications, v. 6, p. 8438, doi:10.1038/ncomms9438.

Mannion, P.D., Upchurch, P., Benson, R.B.J., and Goswami, A., 2014, The latitudinal biodiversity gradient through deep time: Trends in Ecology & Evolution, v. 29, p. 42–50, doi:10.1016/j.tree.2013.09.012.

Markwick, P.J., 1998, Crocodilian diversity in space and time: the role of climate in paleoecology and its implication for understanding K/T extinctions: Paleobiology, v. 24, p. 470–497, doi:10.1017/S009483730002011X.

Markwick, P.J., 2019, Palaeogeography in exploration: Geological Magazine, v. 156, p. 366–407.

Markwick, P.J., 2007, The palaeogeographic and palaeoclimatic significance of climate proxies for data-model comparisons, *in* Williams, M., Haywood, A.M., Gregory, F.J., and Schmidt, D.N.

eds., Deep-Time Perspectives on Climate Change: Marrying the Signal from Computer Models and Biological Proxies, The Geological Society of London on behalf of The Micropalaeontological Society, p. 251–312, doi:10.1144/TMS002.13.

Matthews, K.J., Maloney, K.T., Zahirovic, S., Williams, S.E., Seton, M., and Müller, R.D., 2016, Global plate boundary evolution and kinematics since the late Paleozoic: Global and Planetary Change, v. 146, p. 226–250, doi:10.1016/j.gloplacha.2016.10.002.

McKenzie, D.P., and Parker, R.L., 1967, The North Pacific: an example of tectonics on a sphere: Nature, v. 216, p. 1276–1280.

Merdith, A.S. et al., 2017, A full-plate global reconstruction of the Neoproterozoic: Gondwana Research, v. 50, p. 84–134, doi:10.1016/j.gr.2017.04.001.

Merdith, A.S. et al., 2021, Extending full-plate tectonic models into deep time: Linking the Neoproterozoic and the Phanerozoic: Earth-Science Reviews, v. 214, p. 103477, doi:10.1016/j.earscirev.2020.103477.

Meseguer, A.S., and Condamine, F.L., 2020, Ancient tropical extinctions at high latitudes contributed to the latitudinal diversity gradient: Evolution, p. 1–22, doi:10.1111/evo.13967.

Mitchell, R.N., Kilian, T.M., and Evans, D.A.D., 2012, Supercontinent cycles and the calculation of absolute palaeolongitude in deep time: Nature, v. 482, p. 208–211, doi:10.1038/nature10800.

Morgan, W.J., 1968, Rises, trenches, great faults, and crustal blocks: Journal of Geophysical Research, v. 73, p. 1959–1982.

Müller, R.D. et al., 2019, A Global Plate Model Including Lithospheric Deformation Along Major Rifts and Orogens Since the Triassic: Tectonics, v. 38, p. 1884–1907, doi:10.1029/2018TC005462.

Müller, R.D. et al., 2016, Ocean Basin Evolution and Global-Scale Plate Reorganization Events Since Pangea Breakup: Annual Review of Earth and Planetary Sciences, v. 44, p. 107–138, doi:10.1146/annurev-earth-060115-012211.

Müller, R.D., Cannon, J., Qin, X., Watson, R.J., Gurnis, M., Williams, S., Pfaffelmoser, T., Seton, M., Russell, S.H.J., and Zahirovic, S., 2018, GPlates: Building a Virtual Earth Through Deep Time: Geochemistry, Geophysics, Geosystems, v. 19, p. 2243–2261, doi:https://doi.org/10.1029/2018GC007584.

Müller, R.D., Royer, J.-Y., and Lawver, L.A., 1993, Revised plate motions relative to the hotspots from combined Atlantic and Indian Ocean hotspot tracks: Geology, v. 21, p. 275–278, doi:10.1130/0091-7613(1993)021<0275:RPMRTT>2.3.CO;2.

Powell, M.G., 2009, The Latitudinal Diversity Gradient of Brachiopods over the Past 530 Million Years: The Journal of Geology, v. 117, p. 585–594, doi:10.1086/605777.

Powell, M.G., Moore, B.R., and Smith, T.J., 2015, Origination, extinction, invasion, and extirpation components of the brachiopod latitudinal biodiversity gradient through the Phanerozoic Eon: Paleobiology, v. 41, p. 330–341.

Reddin, C.J., Kocsis, Á.T., and Kiessling, W., 2018, Marine invertebrate migrations trace climate change over 450 million years: Global Ecology and Biogeography, v. 27, p. 704–713, doi:10.1111/geb.12732.

Saupe, E.E., Farnsworth, A., Lunt, D.J., Sagoo, N., Pham, K.V., and Field, D.J., 2019, Climatic shifts drove major contractions in avian latitudinal distributions throughout the Cenozoic: Proceedings of the National Academy of Sciences, v. 116, p. 12895–12900, doi:10.1073/pnas.1903866116.

Scotese, C., 2004, A Continental Drift Flipbook: Journal of Geology, v. 112, p. 729–741, doi:10.1086/424867.

Scotese, C.R., 2016, Tutorial: PALEOMAP paleoAtlas for GPlates and the paleoData plotter program: PALEOMAP Project, Technical Report,.

Scotese, C.R., and Elling, R., 2017, Plate Tectonic Evolution during the last 1.3 billion years: The Movie., *in* Burlington House, London, The Geological Society of London, p. 16–17.

Scotese, C.R., Gahagan, L.M., and Larson, R.L., 1988, Plate tectonic reconstructions of the Cretaceous and Cenozoic ocean basins: Tectonophysics, v. 155, p. 27–48, doi:10.1016/0040-1951(88)90259-4.

Scotese, C.R., Song, H., Mills, B.J.W., and van der Meer, D.G., 2021, Phanerozoic paleotemperatures: The earth's changing climate during the last 540 million years: Earth-Science Reviews, v. 215, p. 103503, doi:10.1016/j.earscirev.2021.103503.

Scotese, C., and Wright, N.M., 2018, PALEOMAP Paleodigital Elevation Models (PaleoDEMs) for the Phanerozoic PALEOMAP Project:, https://www.earthbyte.org/paleodem-resource-scotese-and-wright-2018/.

Seton, M. et al., 2012, Global continental and ocean basin reconstructions since 200 Ma: Earth-Science Reviews, v. 113, p. 212–270, doi:10.1016/j.earscirev.2012.03.002.

Seton, M., Williams, S.E., Domeier, M., Collins, A.S., and Sigloch, K., 2023, Deconstructing plate tectonic reconstructions: Nature Reviews Earth & Environment, p. 1–20, doi:10.1038/s43017-022-00384-8.

Song, H., Huang, S., Jia, E., Dai, X., Wignall, P.B., and Dunhill, A.M., 2020, Flat latitudinal diversity gradient caused by the Permian–Triassic mass extinction: Proceedings of the National Academy of Sciences, p. 1–6, doi:10.1073/pnas.1918953117.

Spano, C.A., Hernández, C.E., and Rivadeneira, M.M., 2016, Evolutionary dispersal drives the latitudinal diversity gradient of stony corals: Ecography, v. 39, p. 836–843, doi:10.1111/ecog.01855.

Torsvik, T.H. et al., 2012, Phanerozoic polar wander, palaeogeography and dynamics: Earth-Science Reviews, v. 114, p. 325–368, doi:10.1016/j.earscirev.2012.06.007.

Torsvik, T.H., and Cocks, L.R.M., 2017, Earth history and palaeogeography:

Torsvik, T.H., Müller, R.D., Van der Voo, R., Steinberger, B., and Gaina, C., 2008a, Global plate motion frames: Toward a unified model: Reviews of Geophysics, v. 46, doi:10.1029/2007RG000227.

Torsvik, T.H., Steinberger, B., Cocks, L.R.M., and Burke, K., 2008b, Longitude: Linking Earth's ancient surface to its deep interior: Earth and Planetary Science Letters, v. 276, p. 273–282, doi:10.1016/j.epsl.2008.09.026.

Torsvik, T.H., and Van der Voo, R., 2002, Refining Gondwana and Pangea palaeogeography: estimates of Phanerozoic non-dipole (octupole) fields: Geophysical Journal International, v. 151, p. 771–794, doi:10.1046/j.1365-246X.2002.01799.x.

Uber, 2023, h3-py: Uber's H3 Hexagonal Hierarchical Geospatial Indexing System in Python:, https://github.com/uber/h3-py.

Vérard, C., 2019, Plate tectonic modelling: review and perspectives: Geological Magazine, v. 156, p. 208–241, doi:10.1017/S0016756817001030.

Vilhena, D.A., and Smith, A.B., 2013, Spatial Bias in the Marine Fossil Record: PLoS ONE, v. 8, p. 1–7, doi:10.1371/journal.pone.0074470.

Williams, S., Cannon, J., Qin, X., and Müller, D., 2017, PyGPlates - a GPlates Python library for data analysis through space and deep geological time: , p. 8556.

Wright, N., Zahirovic, S., Müller, R.D., and Seton, M., 2013, Towards community-driven paleogeographic reconstructions: integrating open-access paleogeographic and paleobiology data with plate tectonics: Biogeosciences, v. 10, p. 1529–1541, doi:10.5194/bg-10-1529-2013.

Young, A., Flament, N., Maloney, K., Williams, S., Matthews, K., Zahirovic, S., and Müller, R.D., 2019, Global kinematics of tectonic plates and subduction zones since the late Paleozoic Era: Geoscience Frontiers, v. 10, p. 989–1013, doi:10.1016/j.gsf.2018.05.011.

Zhang, L., Hay, W.W., Wang, C., and Gu, X., 2019, The evolution of latitudinal temperature gradients from the latest Cretaceous through the Present: Earth-Science Reviews, v. 189, p. 147–158, doi:10.1016/j.earscirev.2019.01.025.

Zhang, S.-H., Shen, S.-Z., and Erwin, D.H., 2022, Latitudinal diversity gradient dynamics during Carboniferous to Triassic icehouse and greenhouse climates: Geology, v. 50, p. 1166–1171, doi:10.1130/G50110.1.

Supplementary information for

MIND THE UNCERTAINTY: GLOBAL PLATE MODEL CHOICE IMPACTS DEEP-TIME PALAEOBIOLOGICAL STUDIES

Lucas Buffan[1,2], Lewis A. Jones[1], Mathew Domeier[3], Christopher R. Scotese[4], Sabin Zahirovic[5], and Sara Varela[1]

[1]*Centro de Investigación Mariña, Grupo de Ecoloxía Animal, Universidade de Vigo, 36310 Vigo, Spain*

[2]*Département de Biologie, École Normale Supérieure de Lyon, Université Claude Bernard Lyon 1, 69342 Lyon Cedex 07, France*

[3]*Centre for Earth Evolution and Dynamics (CEED), University of Oslo, NO-0316 Oslo, Norway*

[4]*Department of Earth and Planetary Sciences, Northwestern University, Evanston, Illinois 60208, USA*

[5]*EarthByteGroup, School of Geosciences, University of Sydney, Sydney, NSW 2006, Australia*

Corresponding authors:

Lucas Buffan (Lucas.L.Buffan@gmail.com) and Lewis A. Jones (LewisAlan.Jones@uvigo.es)

SUPPLEMENTARY TEXT

METHODOLOGICAL BASIS OF GLOBAL PLATE MODELS

Global Plate Models (or Global Plate Rotation Models, GPMs) use the Euler rotation theorem to describe the motion of geometries–such as tectonic plates or geological terranes–on a sphere. A variety of tools have been developed to build global plate tectonic models. However, the most widely used tool is the cross-platform and open-source GPlates (www.gplates.org) software (Boyden et al., 2011; Müller et al., 2018) which is frequently applied to reconstruct the past geographic distribution of fossil samples using various GPMs (e.g. Allen et al., 2020; Boddy et al., 2022; Jones & Eichenseer, 2021).

A GPM is primarily made up of two key components. The first component represents the geometries that define geological boundaries, such as terranes and/or parcels of oceanic crust. GPlates stores these geometries in their present-day positions. Each geometry requires an identity number (Plate ID) and the age at which it first appears. The second component of a GPM is the motion of these geometries through time. This information is stored in a user-editable hierarchical model of finite rotations (Ross & Scotese, 1988) which describes the motion of the geometries through time. GPlates reads and interpolates data from these 'rotation files' to reconstruct the motion of geometries. The most common geometries in GPMs are 'static polygons', otherwise known as 'static plate polygons' or simply 'plate polygons'. Static polygon geometry files are typically made up of numerous polygons which represent individual tectonic plates. While these polygons can rotate across the globe, their shape does not change through time, hence the name static polygons. Each polygon within the geometry file carries a unique Plate ID and a time of appearance (and potentially disappearance) allowing tectonic plates to have an origin and ultimate demise. However, GPMs can have different static polygons (particularly between working groups) and therefore partitioning of the Earth may vary (Fig. S1). Consequently, plate IDs are unique to each static polygon file in GPMs, but they are not necessarily consistent between different GPMs. A specialised variant of plate polygons in plate tectonic modelling are known as continually-closing plate boundaries (Gurnis et al., 2012). These are time-evolving topologies of tectonic plate boundaries (rather than rotated 'static' present-day features), and they approximate the continuous evolution of plate boundaries using a set of dynamically changing plate polygons. This approach was developed to model the relationship between plate evolution and mantle dynamics. More recently, such evolving topological polygons have been expanded to capture deformation in Earth's lithosphere (Gurnis et al., 2018; Müller et al., 2019), which can be used to 'retro-deform' geological sample location (e.g. fossil localities).

Global Plate Modelling requires a 'reference frame' in which the geometries like the plate polygons move. Several reference frames have been proposed, and the types of reference frames being used are extremely important to consider. Fundamentally, 'mantle reference frames' try to isolate the plate-mantle system by eliminating the effect of the centrifugal forces due to Earth rotation on the motion of the 'solid earth' (lithosphere and mantle), namely true polar wander (TPW) (Steinberger & Torsvik, 2008). As both mantellic convection and TPW drive plates motion, removing TPW allows isolation of the plate-mantle system and in turn investigation of the motion of the Earth's outer shell relative to the mantle. For that quality, they are mostly used by the geodynamics and tectonics community. However, removing TPW can have a negative impact upon the reconstruction of palaeocoordinates (i.e. for fossil occurrences or geological samples) (Seton et al., 2023). Therefore, the use of GPMs for palaeoclimatic or palaeobiological studies should carefully consider whether a mantle reference frame is appropriate. For palaeoclimatological and palaeobiological applications, a pure palaeomagnetic reference frame is likely to be more appropriate as it does not eliminate the effects of TPW and is therefore more likely to report true geographic palaeolatitudes.

To constrain the motion of tectonic plates, reference frames are compiling geological data. In particular, palaeolatitudes are robustly estimated using the palaeomagnetic record (i.e. from the inclination of magnetic minerals) (e.g. Beck, 1988; Merdith et al., 2021; Voo, 1993), but due to the radial symmetry of Earth's magnetic field, palaeomagnetic data cannot be used to assess palaeolongitudes. Nevertheless, palaeolongitudinal positioning is possible in a mantle reference frame where a comprehensive set of hot spot tracks can be used to infer the absolute motion of tectonic plates with respect to the base of the mantle (assuming that mantle plumes do not have substantial movement or deflection). Two types of hotspot reference frames have been developed, ones that assume 'fixed hotspots' that do not move (e.g. Müller et al., 1993; Torsvik et al., 2008), and others that incorporate 'moving hotspots' to optimise the fits between hotspot tracks on plates and the source of the hotspots (e.g. O'Neill et al., 2005; Torsvik et al., 2008). The fixed-hotspot reference frame combines palaeomagnetic data with the positional information derived from volcanic hotspots tracks (Müller et al., 1993; Scotese, 2021). However, due the loss of oceanic crust, useful hotspot tracks only extend back until the Early Jurassic. Although (Torsvik et al., 2008) proposed a unifying reference frame constraining palaeolongitude over the last 320 Ma, it is not widely used (Boddy et al., 2022; Merdith et al., 2021).

Though there is currently no method to adequately constrain longitude for intervals prior to 200 Ma, several approaches have been taken to constrain longitudinal positions. A common solution is the 'Africa-fixed' reference frame (Scotese et al., 1988; Torsvik & Cocks, 2016). This approach affixes Africa to the prime meridian (Scotese, 2021) or to a set of active hotspots that surround Africa (Large Low Shear-wave Velocity Provinces) (Torsvik & Cocks, 2016). In these reference frames, Africa remains near the centre of the map, relative longitudinal motions between the plates are preserved and erratic shifts in longitude are eliminated. Another approach is to apply kinematic constraints to minimise trench advance and net rotation, and derive a mantle reference frame that also infers palaeolongitude (Müller et al., 2019, 2022; Tetley et al., 2019).

GPMs are often constructed to address specific applications, such as using mantle reference frames to model mantle convection and isolate the plate-mantle system. However, for the palaeoclimatic and palaeobiological communities, it is crucial to understand what absolute reference frame is used as it may impact upon their reconstructions and subsequent conclusions. In addition to ‘rotation files’, which describe the relative and absolute plate motion paths, the subdivision of Earth’s crust into terranes (or blocks) can also introduce differences in the reconstruction of palaeocoordinates. In most cases, the source of this uncertainty is from varying interpretations of suture zones, where the geological boundaries are typically complex due to prolonged or multiple deformation events. As a result, one should evaluate the impact of GPM choice in relation to their data and understand that each variant carries spatially and temporally evolving uncertainties.

SUPPLEMENTARY REFERENCES

Allen, B. J., Wignall, P. B., Hill, D. J., Saupe, E. E., & Dunhill, A. M. (2020). The latitudinal diversity gradient of tetrapods across the Permo-Triassic mass extinction and recovery interval. *Proceedings of the Royal Society B: Biological Sciences*, *287*(20201125). https://doi.org/10.1098/rspb.2020.1125

Beck, M. E. (1988). Analysis of late Jurassic-recent paleomagnetic data from active plate margins of South America. *Journal of South American Earth Sciences*, *1*(1), 39–52. https://doi.org/10.1016/0895-9811(88)90014-4

Boddy, C. E., Mitchell, E. G., Merdith, A., & Liu, A. G. (2022). Palaeolatitudinal distribution of the Ediacaran macrobiota. *Journal of the Geological Society*, *179*(1), jgs2021-030. https://doi.org/10.1144/jgs2021-030

Boyden, J. A., Müller, R. D., Gurnis, M., Torsvik, T. H., Clark, J. A., Turner, M., Ivey-Law, H., Watson, R. J., & Cannon, J. S. (2011). *Next-generation plate-tectonic reconstructions using GPlates* (G. R. Keller & C. Baru, Eds.; pp. 95–113). Cambridge University Press.

Gurnis, M., Turner, M., Zahirovic, S., DiCaprio, L., Spasojevic, S., Müller, R. D., Boyden, J., Seton, M., Manea, V. C., & Bower, D. J. (2012). Plate tectonic reconstructions with continuously closing plates. *Computers & Geosciences*, *38*(1), 35–42. https://doi.org/10.1016/j.cageo.2011.04.014

Gurnis, M., Yang, T., Cannon, J., Turner, M., Williams, S., Flament, N., & Müller, R. D. (2018). Global tectonic reconstructions with continuously deforming and evolving rigid plates. *Computers & Geosciences*, *116*, 32–41. https://doi.org/10.1016/j.cageo.2018.04.007

Jones, L. A., & Eichenseer, K. (2021). Uneven spatial sampling distorts reconstructions of Phanerozoic seawater temperature. *Geology*. https://doi.org/10.1130/G49132.1

Merdith, A. S., Williams, S. E., Collins, A. S., Tetley, M. G., Mulder, J. A., Blades, M. L., Young, A., Armistead, S. E., Cannon, J., Zahirovic, S., & Müller, R. D. (2021). Extending full-plate tectonic models into deep time: Linking the Neoproterozoic and the Phanerozoic. *Earth-Science Reviews*, *214*, 103477. https://doi.org/10.1016/j.earscirev.2020.103477

Müller, R. D., Cannon, J., Qin, X., Watson, R. J., Gurnis, M., Williams, S., Pfaffelmoser, T., Seton, M., Russell, S. H. J., & Zahirovic, S. (2018). GPlates: Building a Virtual Earth Through Deep Time. *Geochemistry, Geophysics, Geosystems*, *19*(7), 2243–2261. https://doi.org/10.1029/2018GC007584

Müller, R. D., Flament, N., Cannon, J., Tetley, M. G., Williams, S. E., Cao, X., Bodur, Ö. F., Zahirovic, S., & Merdith, A. (2022). A tectonic-rules-based mantle reference frame since 1 billion years ago – implications for supercontinent cycles and plate–mantle system evolution. *Solid Earth*, *13*(7), 1127–1159. https://doi.org/10.5194/se-13-1127-2022

Müller, R. D., Royer, J.-Y., & Lawver, L. A. (1993). Revised plate motions relative to the hotspots from combined Atlantic and Indian Ocean hotspot tracks. *Geology*, *21*(3), 275–278. https://doi.org/10.1130/0091-7613(1993)021<0275:RPMRTT>2.3.CO;2

Müller, R. D., Zahirovic, S., Williams, S. E., Cannon, J., Seton, M., Bower, D. J., Tetley, M. G., Heine, C., Le Breton, E., Liu, S., Russell, S. H. J., Yang, T., Leonard, J., & Gurnis, M. (2019). A Global Plate Model Including Lithospheric Deformation Along Major Rifts and Orogens Since the Triassic. *Tectonics*, *38*(6), 1884–1907. https://doi.org/10.1029/2018TC005462

O'Neill, C., Müller, D., & Steinberger, B. (2005). On the uncertainties in hot spot reconstructions and the significance of moving hot spot reference frames. *Geochemistry, Geophysics, Geosystems*, *6*(4). https://doi.org/10.1029/2004GC000784

Ross, M. I., & Scotese, C. R. (1988). A hierarchical tectonic model of the Gulf of Mexico and Caribbean region. *Tectonophysics*, *155*(1), 139–168. https://doi.org/10.1016/0040-1951(88)90263-6

Scotese, C. R. (2021). An Atlas of Phanerozoic Paleogeographic Maps: The Seas Come In and the Seas Go Out. *Annual Review of Earth and Planetary Sciences*, *49*(1), 679–728. https://doi.org/10.1146/annurev-earth-081320-064052

Scotese, C. R., Gahagan, L. M., Royer, J.-Y., Mueller, R. D., Ross, M. I., Nurnberg, D., Mayes, C. L., Lawver, L. A., Tomlins, R., & Beckley, L. (1988). Phanerozoic plate tectonic reconstructions. *Geological Society of America, Centennial Celebrations, Abstracts with Programs*, *20*, 229.

Seton, M., Williams, S. E., Domeier, M., Collins, A. S., & Sigloch, K. (2023). Deconstructing plate tectonic reconstructions. *Nature Reviews Earth & Environment*, 1–20. https://doi.org/10.1038/s43017-022-00384-8

Steinberger, B., & Torsvik, T. H. (2008). Absolute plate motions and true polar wander in the absence of hotspot tracks. *Nature*, *452*(7187), Article 7187. https://doi.org/10.1038/nature06824

Tetley, M. G., Williams, S. E., Gurnis, M., Flament, N., & Müller, R. D. (2019). Constraining Absolute Plate Motions Since the Triassic. *Journal of Geophysical Research: Solid Earth*, *124*(7), 7231–7258. https://doi.org/10.1029/2019JB017442

Torsvik, T. H., & Cocks, L. R. M. (2016). *Earth history and palaeogeography* (Cambridge University Press).

Torsvik, T. H., Müller, R. D., Van der Voo, R., Steinberger, B., & Gaina, C. (2008). Global plate motion frames: Toward a unified model. *Reviews of Geophysics*, *46*(3). https://doi.org/10.1029/2007RG000227

Voo, R. van der. (1993). *Paleomagnetism of the Atlantic, Tethys and Iapetus Oceans*. Cambridge University Press. https://doi.org/10.1017/CBO9780511524936

SUPPLEMENTARY FIGURES

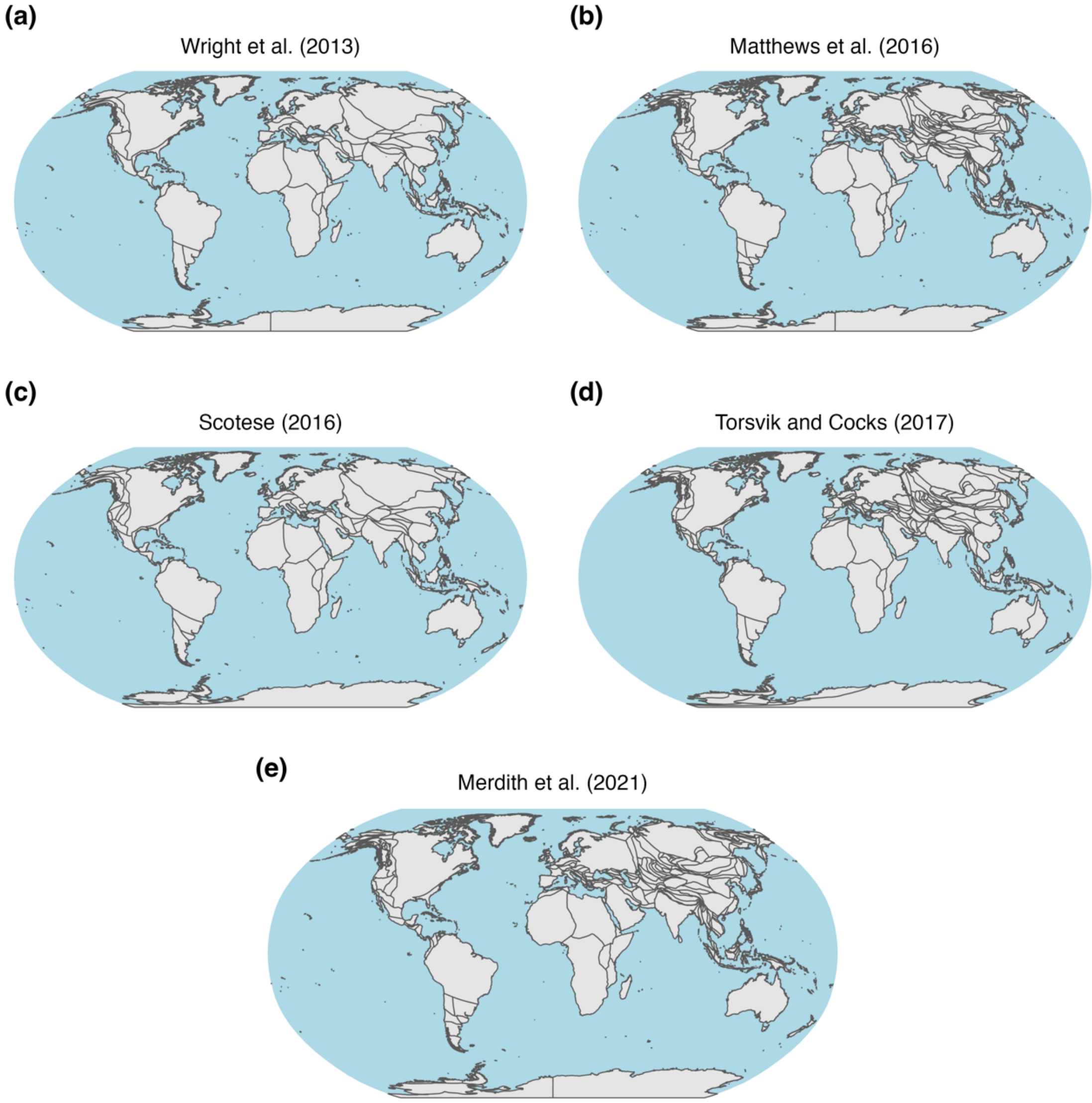

Figure S1: Continental plate polygons for Global Plate Models used in this study. Note: Global Plate Models partition continental plate polygons differently, including where polygons are partitioned, and how many partitions are present. Maps are presented in the Robinson projection (ESRI:54030).

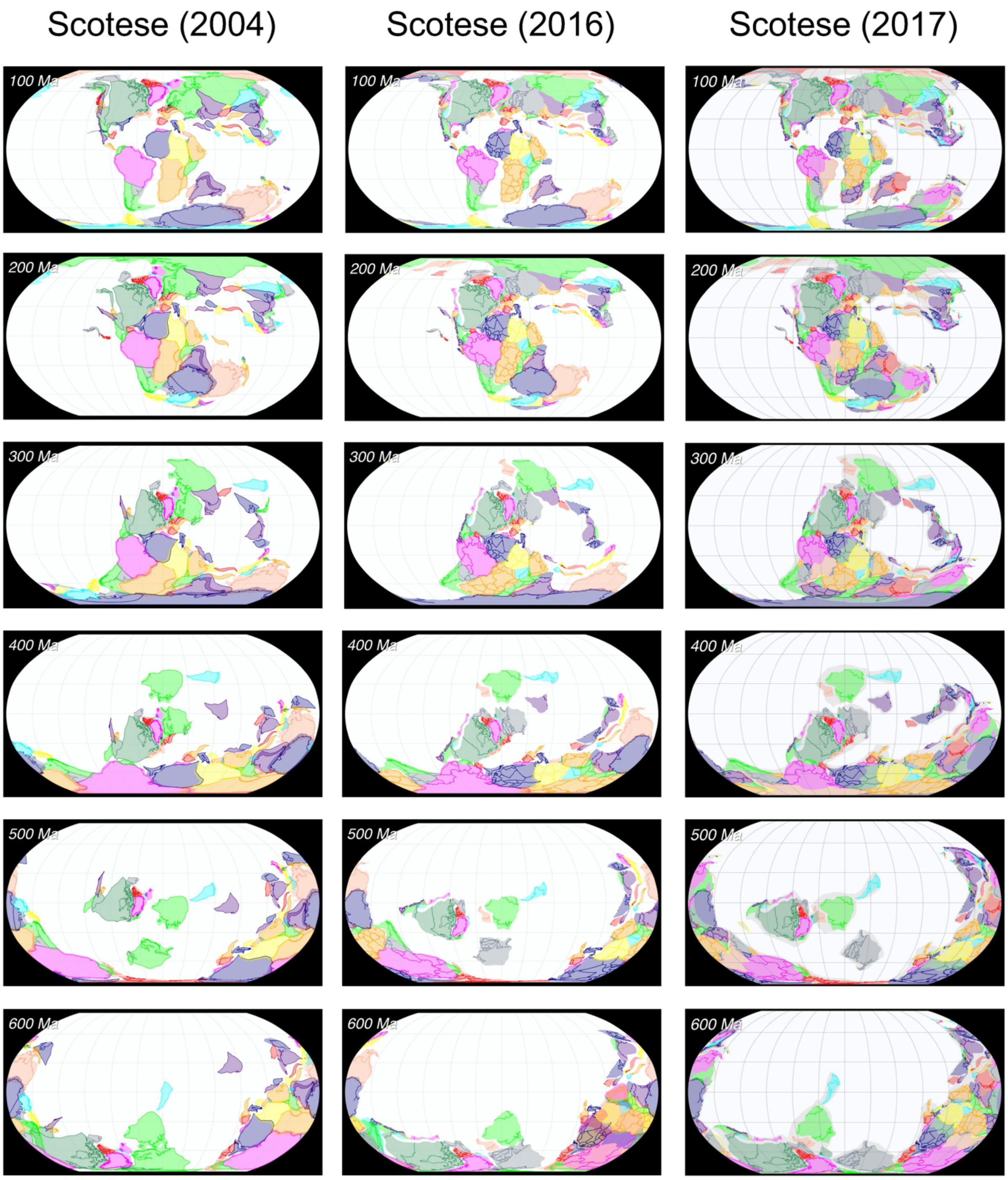

Figure S2: Evolution of the Scotese Global Plate Model (2004–2017). Small changes occur in the location of the 'core' continents. Major changes occur in the placement of N. China, S. China, Cimmeria, and the exotic terranes of western North America. The time range of the models has also evolved (though not fully depicted here), with Scotese (2004) ranging from 0–750 Ma, Scotese (2016) from 0–1100 Ma, and Scotese (2017) from 0–1500 Ma. Maps are presented in the Robinson projection (ESRI:54030).

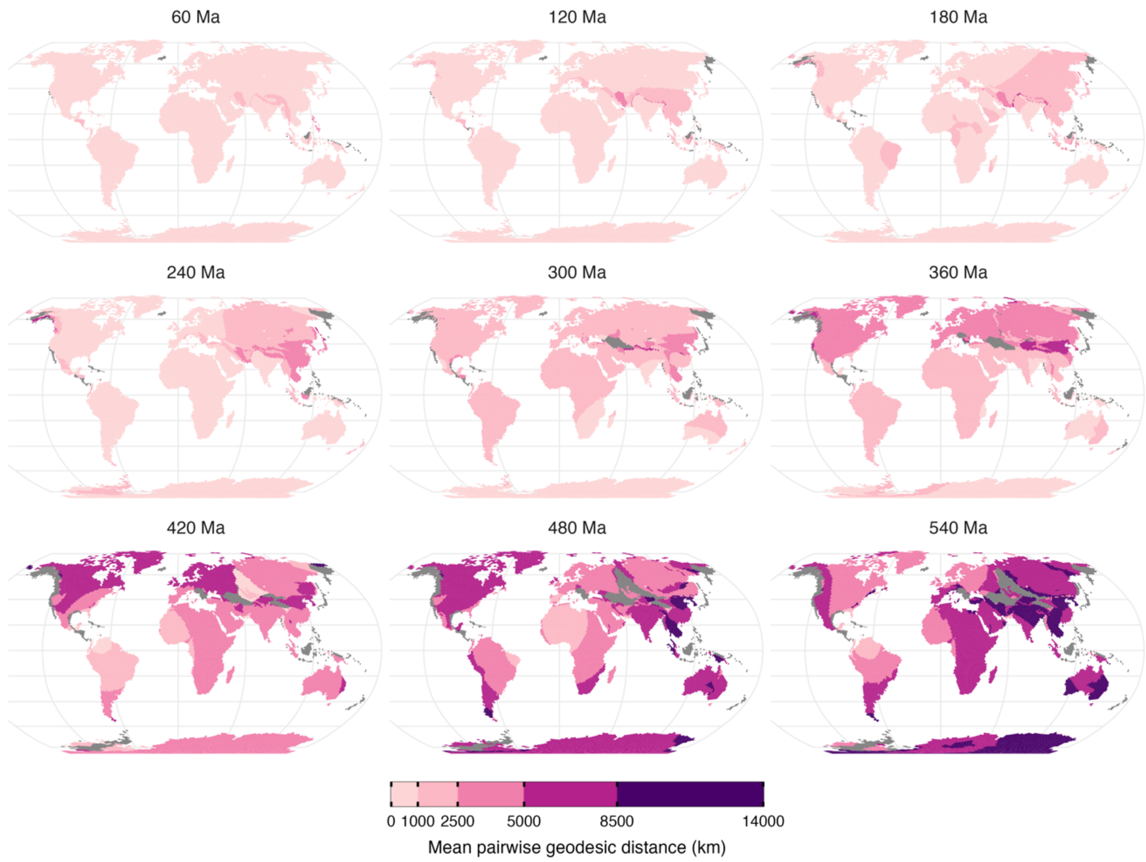

Figure S3. Categorised maps of the mean pairwise geodesic distance between reconstructed palaeocoordinates of cell centroids from Global Plate Models. Values are mapped onto a present-day map with darker shades indicating greater geographic distance between palaeocoordinates. Grey cells denote areas where palaeocoordinates could not be reconstructed at time of reconstruction for cell centroids by at least two models. Maps are presented in the Robinson projection (ESRI:54030).

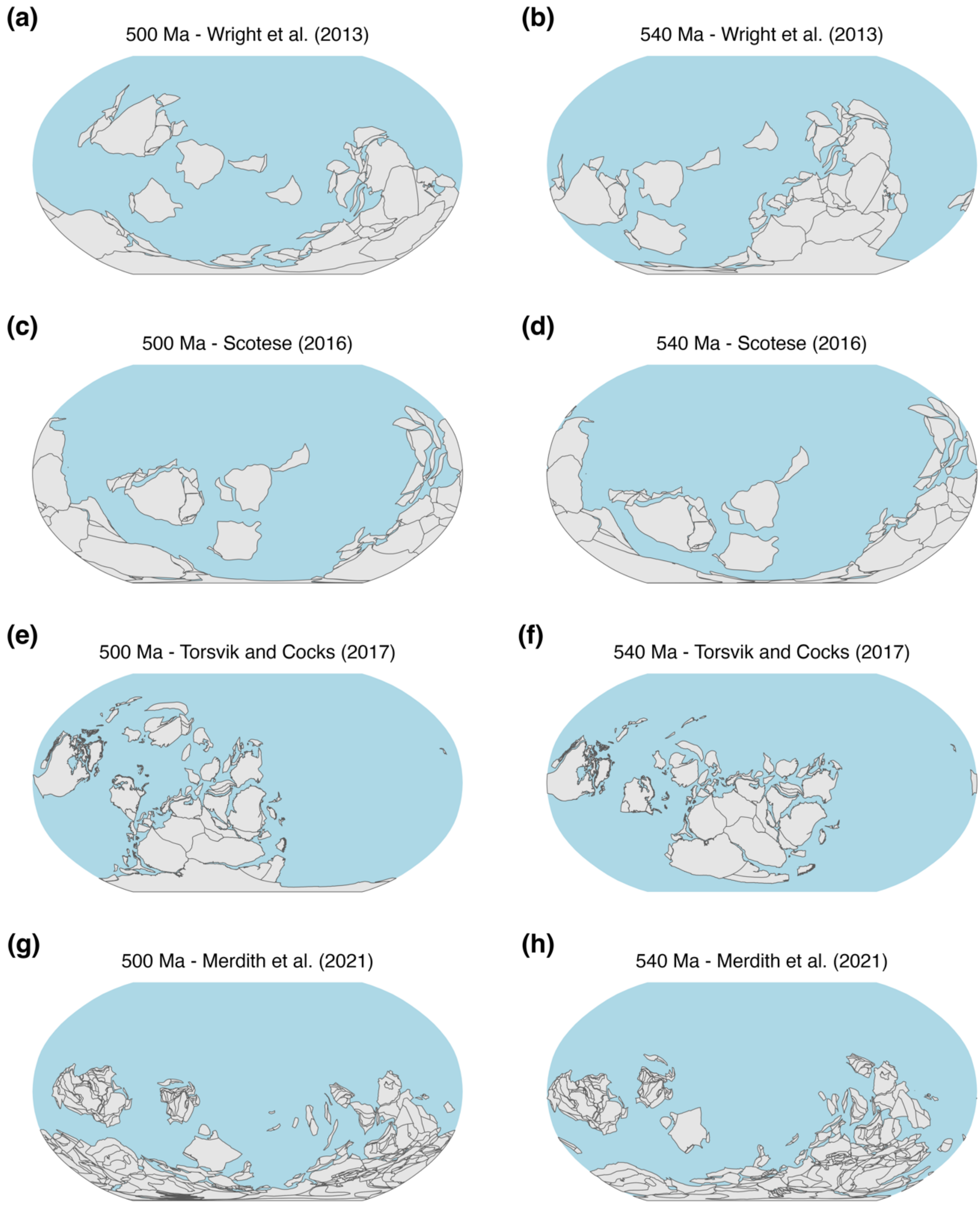

Figure S4: Reconstructed continental areas of the early and late Cambrian according to different Global Plate Models: WR13 (a, b), SC16 (c, d), TC17 (e, f) and ME21 (g, h). The left-hand side of the panel depicts palaeogeographic reconstructions of the Earth at 500 Ma (early Cambrian). The right-hand side of the panel depicts palaeogeographic reconstructions of the Earth at 540 Ma (late Cambrian). The MA16 Global Plate Model is not depicted here as the Cambrian is not within its temporal coverage. Maps are presented in the Robinson projection (ESRI:54030).

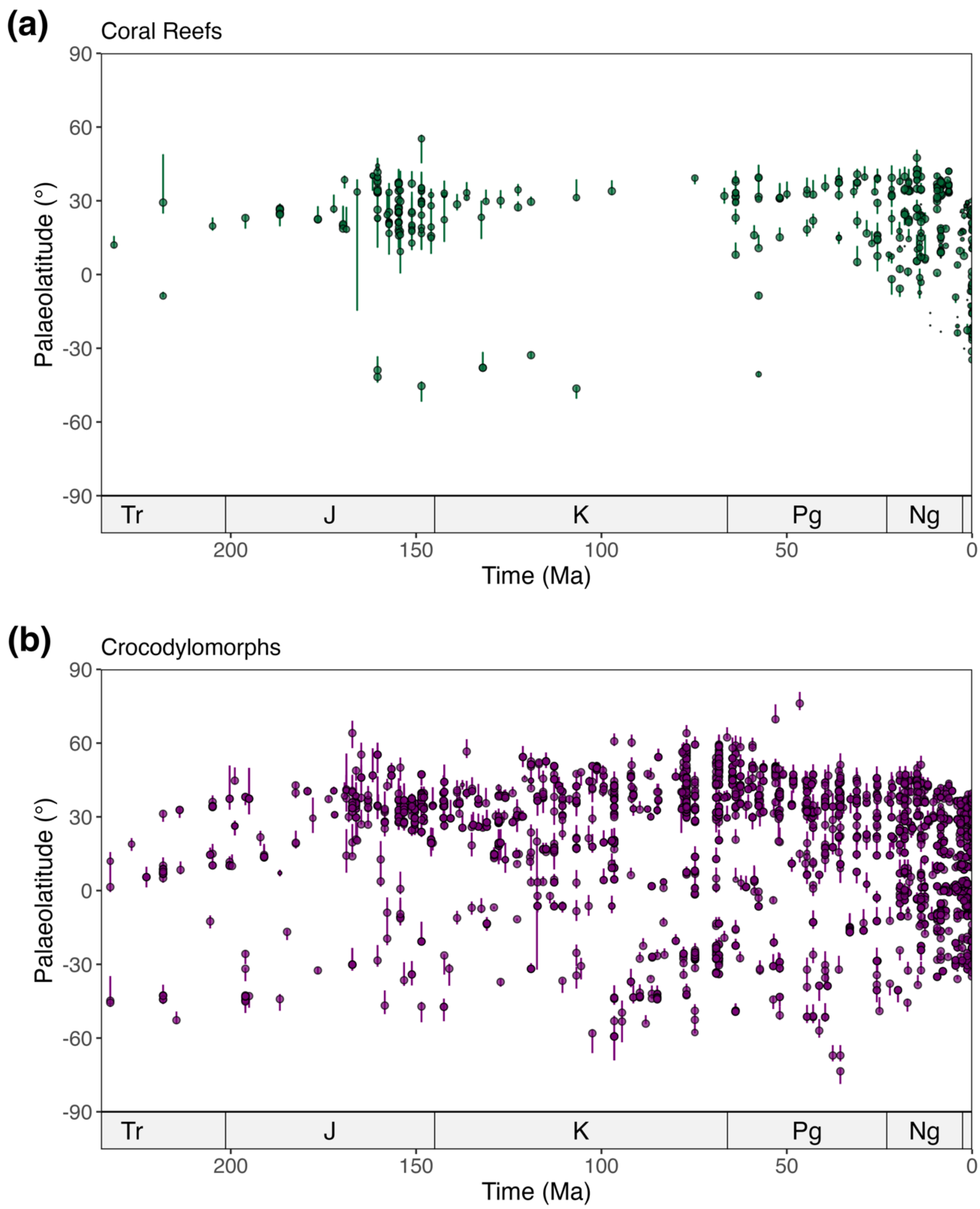

Figure S5: Palaeolatitudinal reconstruction of fossil coral reefs (a) and terrestrial crocodylomorphs (b) according to the five Global Plate Models used in this study. Each point represents the median of the palaeolatitude estimate for an occurrence. The size of the points is proportional to the logarithm of the number of models palaeocoordinates could be reconstructed from (n = 1 to 5). Each bars depict the minimum and maximum palaeolatitudinal estimate for an occurrence. Pearson's correlation tests showed significant positive relations between the age of reconstruction and average range of palaeolatitudinal estimates per time interval (R = 0.33–0.49; $P < 0.001$).